Vol. 677: 209–217, 2021
https://doi.org/10.3354/meps13866

MARINE ECOLOGY PROGRESS SERIES
Mar Ecol Prog Ser

Published October 28

Size and body condition of sympatric killer whale ecotypes around the Antarctic Peninsula

J. W. Durban[1,2,*], H. Fearnbach[3], A. Paredes[3], L. S. Hickmott[4], D. J. LeRoi[5]

[1]Marine Mammal and Turtle Division, Southwest Fisheries Science Center, National Marine Fisheries Service, 8901 La Jolla Shores Drive, La Jolla, CA 92037, USA

[2]Southall Environmental Associates, Inc., 9099 Soquel Dr., Aptos, CA 95003, USA

[3]SR[3] SeaLife Response, Rehabilitation, and Research, 2003 S. 216th St. #98811, Des Moines, WA 98198, USA

[4]Open Ocean Consulting, 3B Oaklands Road, Petersfield GU32 2EY, UK

[5]Aerial Imaging Solutions, 5 Myrica Way, Old Lyme, CT 06371, USA

ABSTRACT: Killer whales *Orcinus orca* are apex predators, and their health can indicate trophic dynamics in ecosystems that support them. We used aerial photogrammetry to estimate body lengths, to better understand size differences and food requirements, and widths, to infer current nutritional condition, of killer whales in the rapidly warming waters around the Antarctic Peninsula. A remotely controlled hexacopter drone was used to collect aerial images of 242 killer whales of 3 sympatric ecotypes (Type A, n = 34; Type B1, n = 19; and Type B2, n = 189) in the austral summers between 2015/2016 and 2018/2019. Total length (TL) varied between ecotypes, with B2s being diminutive in size, indicating large differences in energy requirements. The mean length for adult females ranged from 5.82 m (B2s) to 6.93 m (B1s), and the mean for adult males ranged from 6.44 m (B2s) to 7.80 m (As). We also found significant differences in head width (HW, proxy for body condition), with B2s being significantly leaner. Although this variation may reflect natural shape differences, we also estimated divergent regression lines of HW~TL indicating that this difference was greater at larger body sizes, with some anomalously thin adult female B2s. We suggest that these dissimilarities may indicate a density-dependent response, with leaner body condition in adults with higher energetic requirements, as the abundance of B2s is almost an order of magnitude greater than that of B1s and As. We hypothesize that food limitation resulted from a decline in carrying capacity during recent reductions in sea ice and warmer ocean temperatures.

KEY WORDS: Photogrammetry · Drone · Antarctica · Climate change · Predator · Marine mammal

1. INTRODUCTION

Killer whales *Orcinus orca* are apex marine predators known to have high caloric requirements (Noren 2011) and therefore show population responses to changes in prey availability (Ford et al. 2010). Consequently, studies of killer whales may help understand the impact of physical and biological ecosystem changes by measuring their responses to trophic dynamics in the ecosystem that supports them. The marine environment around the Antarctic Peninsula (AP) is under acute transition, with climate warming leading to changes in the physical marine environment and biology, and interacting with an increase in human activities (Convey & Peck 2019, Gutt et al. 2021). Here we report on the use of aerial photogrammetry to estimate body lengths, to better understand size differences and resultant food requirements, and body widths, to infer current nutritional condition, of killer whales in this changing system. Notably, our study in the austral summers of 2015/16 to 2018/19 overlapped with a period of significant reduction in

*Corresponding author: john.durban@sea-inc.net

Publisher: Inter-Research · www.int-res.com

sea ice and associated ocean warming in the Weddell Sea, which extended to our sampling areas off the northern and western AP (Turner et al. 2020). Specifically, in the austral summer of 2016/17, the sea ice extent dropped to near-record low levels (second lowest in a 40 yr record) and remained at near-record low levels for the remaining 2 summers of our study (Turner et al. 2020).

A growing body of data is defining 3 generally sympatric ecotypes of killer whales around the AP, which are distinct both morphologically (Pitman & Ensor 2003, Durban et al. 2017) and genetically (Morin et al. 2010, 2015, Foote et al. 2016). Notably, these ecotypes have varying ecology and trophic interactions. Type A ranges widely in the Southern Ocean and is using AP coastal waters in increasing abundance, taking advantage of increasingly ice-free waters to prey on marine mammals (Fearnbach et al. 2019). In contrast, the uniquely pigmented Type Bs (2 ecotypes) are endemic to Antarctica, with the exception of rapid return migrations to the subtropics that are thought to be for physiological maintenance and skin growth in warmer waters (Durban & Pitman 2012, Pitman et al. 2020). Similarly, their physiology is adapting to the extreme cold in Antarctica (Foote et al. 2011, 2016) enabling 2 divergent ecotypes (Durban et al. 2017) to occur year-round in the coastal waters of the AP: Type B1 specializes in hunting seals that haul out on pack ice (Pitman & Durban 2012), while individuals of Type B2 are generally found in more open water where they feed on penguins (Pitman & Durban 2010) and occasionally Weddell seals *Leptonychotes weddellii* (B. Pitman unpubl. data) and regularly undertake prolonged bouts of deep diving (regular dives of 500–700 m, Pitman et al. 2020), likely to feed on fish.

Photographic mark–recapture estimates suggest recent population responses of these killer whale ecotypes that are plausibly related to climate-driven declines in sea ice around the AP (Fearnbach et al. 2019, 2021). Specifically, a population decline of the most pagophilic Type B1 contrasts with abundance increases in Type A killer whales that prefer open water. This is similar to the contrasting abundance changes of different penguin species off the western AP, which has seen an abrupt decline in the breeding population of ice-obligate Adélie penguins *Pygoscelis adeliae* and an abrupt increase in ice-intolerant gentoo penguins *P. papua* (Bestelmeyer et al. 2011). There are also emerging indications of a change in population health of Type B2 killer whales, the most abundant ecotype around the AP. Specifically, despite being generally stable in abundance and survival over the past decade, Fearnbach et al. (2021) reported a year of anomalously low survival in 2016–2017, but it is not yet clear if this is a continuing trend. Unfortunately, the inherent uncertainty of sampling-based whale population estimates limits statistical power and requires long time series to detect further trends at the population level (Gerrodette 1987).

As an alternative, photogrammetry measures of individual body condition have recently been shown to offer high statistical power to detect changes in nutritional health of killer whales (Fearnbach et al. 2020). For these long-lived top predators, such measures can be predictive of future mortality risk and therefore can provide an early warning of impending population effects (Stewart et al. 2021a). In this context, we used photographs from a remotely controlled drone (Durban et al. 2015) to generate photogrammetric measurements of body width to infer the condition of all 3 killer whale ecotypes and provide a baseline for future monitoring. While body condition informs on current nutritional status and population health, we also provide estimates of body length for each type that represent key data for parameterization of energetic models for understanding prey requirements (Noren 2011).

2. MATERIALS AND METHODS

Aerial images of killer whales around the AP were collected in the austral summer (January to February) in each of 4 different years, from 2015/16 to 2018/19. Encounters occurred mostly in the coastal waters close to the west side of the AP, but also to the northeast of the AP in the far western Weddell Sea (Fig. 1). We launched and recovered a remotely controlled hexacopter drone (APH-22 Aerial Imaging Solutions; Durban et al. 2015, 2016) by hand from a small (5.85 m) inflatable boat that approached killer whales within a typical distance of 200 m. Individual whales were distinguished based on distinctive pigmentation and scarring patterns that were visible in the aerial images (e.g. Durban et al. 2015, Groskreutz et al. 2019). Whales were assigned to Type A, B1 or B2 based on characteristic pigmentation patterns that were visible in aerial photographs and corroborated by boat-based observations and photographs (Fig. 2 and see Fig. 4; Pitman & Ensor 2003, Durban et al. 2017, Fearnbach et al. 2019). Reliable assignments of type in the field and in subsequent photographs by the authors have been repeatedly corroborated by genetic analyses (Morin et al. 2010, 2015, Foote et al. 2016).

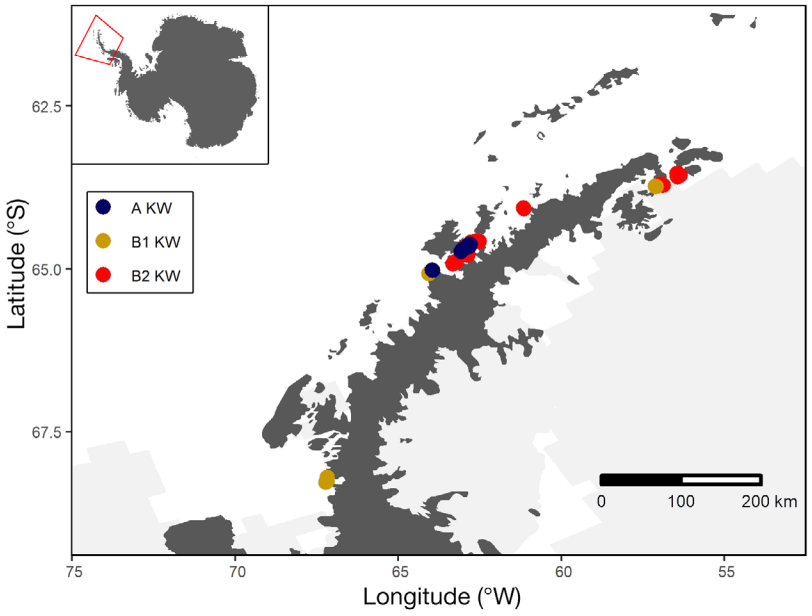

Fig. 1. Antarctic Peninsula showing locations of 96 flights with a remotely controlled hexacopter drone to obtain aerial images of Type A, B1 and B2 killer whales. Light gray shows ice sheets and sea ice as a daily average for the month of January 2018

During each year, a micro 4/3 digital camera (Olympus E-PM2) and flat lens (25 mm F1.8 Olympus M. Zuiko) were mounted on a powered gimbal to collect vertical images from altitudes of 22–48 m to provide a water-level pixel resolution of 1–2 cm (Durban et al. 2015). Pixel measurements of killer whale morphometrics were converted to distance units using their ratio to the known size of the camera sensor (4608 pixels = 17.3 mm wide) and were then scaled to true size (scale = altitude/focal length) using altitude measured by an onboard temperature-compensated pressure altimeter (Durban et al. 2015). Because the killer whales often did not surface with their entire body parallel to the water's surface, total length (TL) estimates for each individual were derived from the addition of the maximum measurements across repeat images for the tip of the rostrum to the anterior of the dorsal fin and the anterior insertion of the dorsal fin to the fluke notch; this summation was assumed to represent the flattest measurement of an individual that would be closest to true length (Groskreutz et al. 2019).

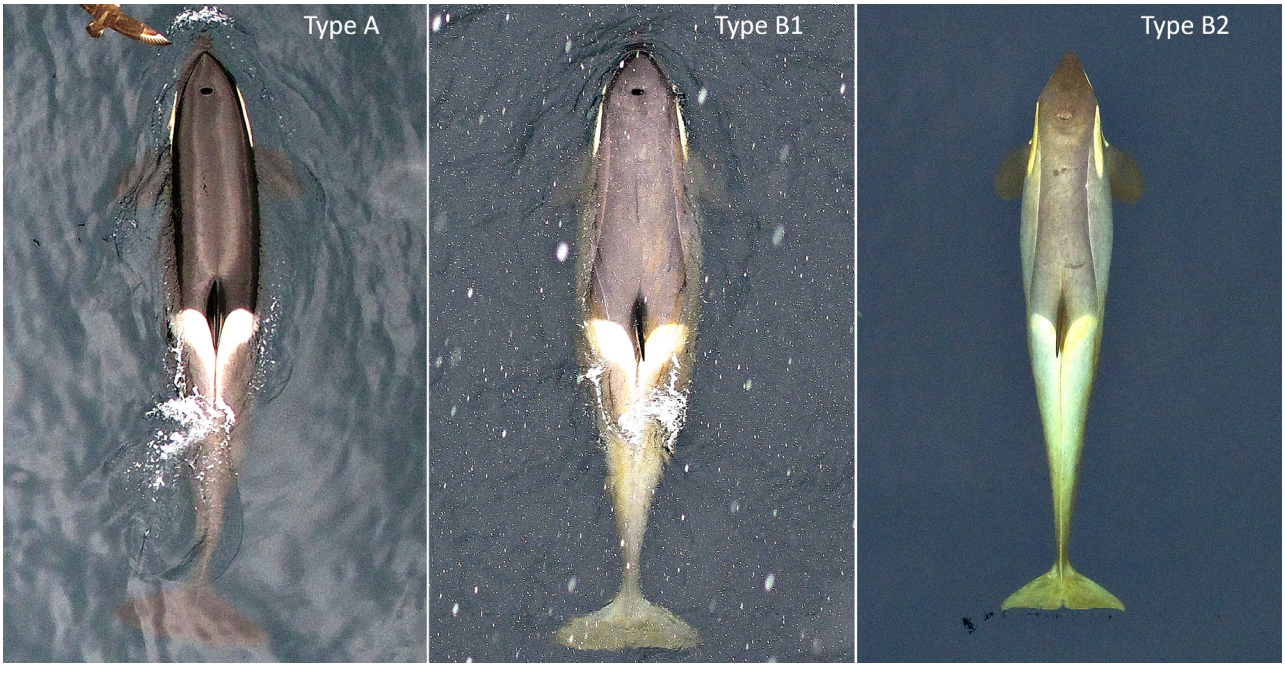

Fig. 2. Aerial images of killer whales of the 3 ecotypes (A, B1 and B2) in the coastal waters of the Antarctic Peninsula. All are adult females in relatively good body condition for their ecotype; the yellow hue on Type B1 and B2 reflects diatoms on the skin (see Durban & Pitman 2012). Images collected using a remotely controlled hexacopter at altitudes of ~30 m, scaled to whale size using camera focal length and altitude estimated from an onboard pressure altimeter (Durban et al. 2015)

To make consistent comparisons of TL between killer whale ecotypes, we identified adult females as those with small calves traveling in echelon position and adult males based on visible secondary sexual characteristics of enlarged pectoral fins and curved tail flukes (Fig. 3). To assess differences in the TLs of these confirmed males and females, within and between ecotypes, we adopted a Bayesian formulation of a fixed-effects ANOVA model (Kerry 2010). Uniform prior distributions were placed on the mean lengths for each sex–ecotype grouping and on the residual standard deviation (SD) away from the group means. These parameters were estimated by fitting to the TL of each individual in each group using Markov chain Monte Carlo (MCMC) sampling using the package 'Nimble' (de Valpine et al. 2020) in the R statistical environment (R version 3.6.1; www.r-project.org). The probability of whales in one group having longer lengths than another (e.g. $p[mean\_TL^{malesB1} > mean\_TL^{malesB2}]$) was simply derived from the proportion of MCMC samples where the difference in parameter estimates was greater than zero.

To quantify body condition, we measured the head width (HW) for all whales at a distance of 15% between the center of the blowhole and anterior insertion of the dorsal fin. Reduced fat storage behind the cranium is an obvious measure of poor condition in cetaceans and can result in a 'peanut head' appearance that is particularly visible in aerial images of killer whales (Fig. 3; Fearnbach et al. 2018). By examining aerial images of emaciated killer whales, this HW measure was identified as a useful proxy for body condition, and has been shown to reveal significant changes over time (Fearnbach et al. 2018). Recognizing that HW changes with body growth (Fearnbach et a. 2020), we interpreted the median HW for each individual in a regression against TL to compare the intercept and slope of separate regression lines for each ecotype. We centered each regression on a TL of 6 m, so the intercept provided a comparative HW measure at TL = 6 m for each type. We adopted a Bayesian formulation to make comparisons using direct probability statements, and used non-informative uniform prior distributions on the intercepts, slopes and residual SDs around the regression lines. We calculated the probability that a given whale was an abnormal outlier with a residual of more than 2 SDs (i.e. 2 times the average residual) on either side of its ecotype regression line using the Bayesian approach of Chaloner &

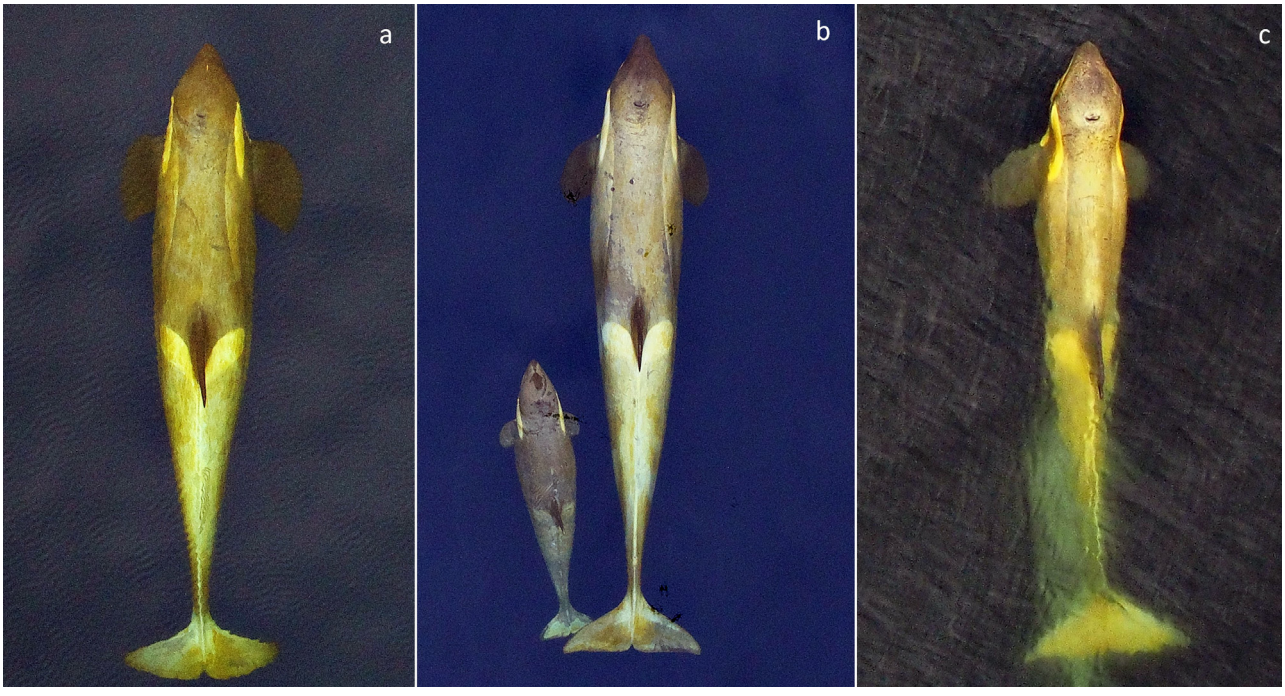

Fig. 3. Aerial images of Type B2 killer whales in the coastal waters of the Antarctic Peninsula. (a) Adult male, identified based on visible secondary sexual characteristics of enlarged pectoral fins and curved tail flukes. (b) Adult female with a small calf in echelon position. (c) Clearly emaciated adult female displaying the 'peanut head' condition (one of the outliers in Fig. 5 and Table 2), with her dependent calf swimming beneath her. Images collected using a remotely controlled hexacopter drone at altitudes of ~30 m, scaled to whale size using camera focal length and altitude from an onboard pressure altimeter (Durban et al. 2015). The yellow hue reflects diatoms on the skin (see Durban & Pitman 2012)

Brant (1988). The 3 ecotype regression models were fit simultaneously using MCMC sampling in the package 'Nimble' (de Valpine et al. 2020) in R (version 3.6.1), and the probability of one regression parameter being greater than an another (e.g. $p[slope^{B1} > slope^{B2}]$) was derived from the proportion of MCMC samples where the difference in parameter estimates was greater than zero.

3. RESULTS

From 2016 to 2019, we flew 96 hexacopter flights over killer whales (Table 1), each lasting an average of 9 min (max = 12 min). Measurements of 45 calibration images of a known-length rail on the research boat were also taken on 20 d over all 4 years, and revealed the system to be approximately unbiased with an average error of <0.01 m. The SD in error was 3.6% (0.11 m compared to 2.95 m rail). We collected 3065 measurement-quality images of 242 different killer whales comprising all 3 types (Fig. 2, Table 1), including both adult males and adult females of each type (Fig. 3). Type B2s were imaged in all 4 years of the study, B1s in 3 years and As in 2 different years (Table 1). Estimates of TL were derived from an average (median) of 8 measurements of the tip of the rostrum to anterior insertion of the dorsal fin per individual (range = 1–23) combined with a median of 6 (1–29) measurements of the anterior insertion of the dorsal fin to the fluke notch. Body condition was inferred from a median of 6 (1–19) measurements of HW for each individual. Variability in repeat measurements of the same whale was low, with a mean coefficient of variation (= SD/mean) of <5% for both TL and HW.

There were notable differences in TL estimates between types (Table 2, Fig. 4). Confirmed adults of Types A and B1 were of similar sizes, but the ANOVA estimated moderate probabilities of 0.89 and 0.88 for length differences between males and females, respectively, of these types. It was noteworthy that the largest males were Type A (mean = 7.80 m, max = 8.92 m) but the largest females were Type B1 (mean = 6.93 m, max = 7.36 m). In contrast, Type B2 individuals were diminutive in length with high probabilities (p = 1 in all cases) of length differences of male and female B2s compared to both other ecotypes. Type B2 males were 1.36 m shorter than Type A males on average, and females were 1.11 m shorter than Type B1 females. There was a high probability (p = 1) of males being longer than females for all ecotypes. This sexual dimorphism was most prominent in Type As, with the average male being 1.04 m longer than the average female, compared to only 0.65 and 0.62 m for Types B1 and B2, respectively.

Differences in length translated to differences in HW, with the smaller Type B2s having narrower heads (Fig. 5). However, the regression of HW against TL revealed significant differences in HW when accounting for length (Table 2), with high probabilities (p = 1 in both cases) that the intercept of HW at TL = 6 m for B2s was thinner than that of both As and B1s, respectively. In contrast, there was no evidence (p = 0.42) that Type As were wider than B1s at TL = 6 m. There were also differences in the slopes of the HW~TL relationships, with the steepest slope for Type B1s (p = 0.91 that it was steeper than Type As and p = 0.99 that it was steeper than B2s) indicating that they became significantly more robust with increasing length, particularly in relation to Type B2s. Type B2s had the shallowest slope, with p > 0.90 that it was in turn shallower than Type As, indicating that their proportionally leaner body condition was more pronounced as TL increased. Supporting inference of their comparative poor condition, 8 Type B2 whales measured between 2016 and 2018 were identified as significant outliers (Table 2), and 6 of these had anomalously lean heads with HW below the regression line (3 in 2016, 1 in 2017 and 2 in 2018;

Table 1. Summary of drone-derived aerial images collected in the coastal waters of the Antarctic Peninsula to estimate length and body condition for Type A, B1 and B2 killer whales using photogrammetry analyses. Data shown for each year (2016–2019) are the range (min–max) of sampling dates (month/day), range (min–max) of locations, number and total minutes of drone flights and the number of different individuals imaged for each ecotype

Year	Dates	Latitude (°S)	Longitude (°W)	Flights (min)	Number of individuals		
					Type A	Type B1	Type B2
2016	1/12–1/25	64.1–64.6	61.1–62.8	7 (73)	0	0	59
2017	1/24–2/14	63.7–64.8	56.9–63.1	43 (389)	28	7	54
2018	1/20–2/3	64.6–68.3	63.5–67.2	18 (119)	0	5	22
2019	2/2–2/12	63.5–65.1	56.4–64.1	28 (226)	6	7	54

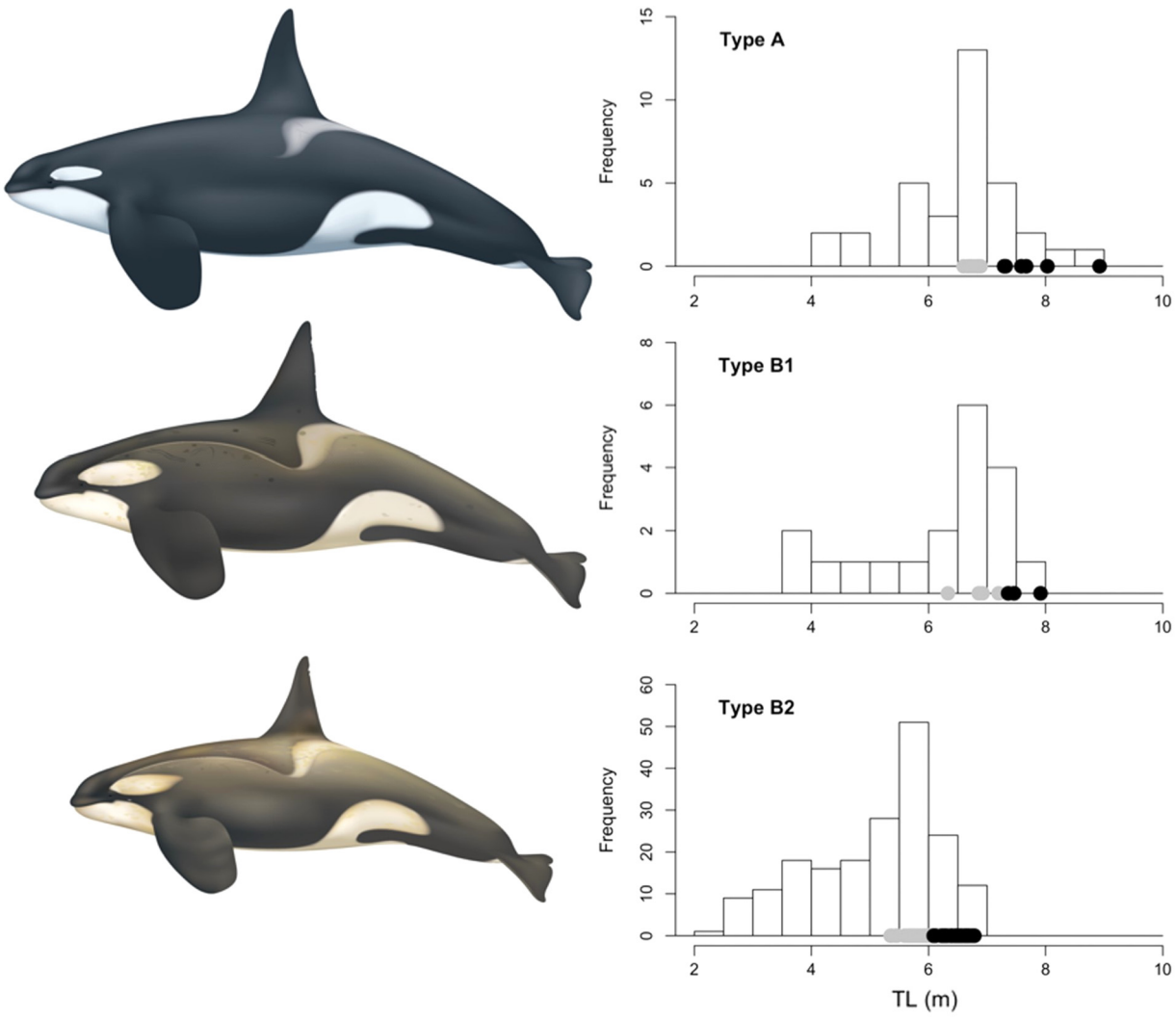

Fig. 4. Distributions of total length (TL) estimates for Type A, B1 and B2 killer whales from photogrammetry analysis of aerial images collected in the coastal waters of the Antarctic Peninsula. TLs for adult males (females) are shown by black (gray) circles. Illustrations by Uko Gorter, scaled to the mean TL estimates of adult males for each type (Table 1)

Table 2. Summary of length and body condition parameters for Type A, B1 and B2 killer whales from photogrammetry analysis of aerial images collected in the coastal waters of the Antarctic Peninsula. The sample size n of all whales is shown, along with the mean total length (TL), standard deviation (SD) and sample sizes for confirmed adult females (fem) and adult males of each type. A linear model of head width (HW, proxy for body condition) against TL for all whales produced parameters for intercept (HW_int) that represented HW at a TL = 6 m, a slope (HW_slope) and a residual SD about the trendline (HW_resid); these parameters are presented as medians of Bayesian posterior distributions along with 95% highest posterior probability intervals (PI). Outliers are whales that had a high probability ($p > 0.75$) of a residual of >2 SD on either side of the regression line

Type	n (total)	TL_{fem} (m) (n, SD)	TL_{male} (m) (n, SD)	HW_int (95% PI)	HW_slope (95% PI)	HW_resid (95% PI)	Outliers
A	34	6.76 (10, 0.09)	7.80 (6, 0.61)	0.78 (0.77, 0.80)	0.09 (0.08, 0.11)	0.04 (0.04, 0.05)	1
B1	19	6.93 (6, 0.35)	7.58 (3, 0.29)	0.78 (0.76, 0.80)	0.11 (0.09, 0.13)	0.05 (0.04, 0.07)	1
B2	189	5.82 (35. 0.21)	6.44 (24, 0.22)	0.68 (0.67, 0.69)	0.08 (0.08, 0.09)	0.04 (0.03, 0.04)	8

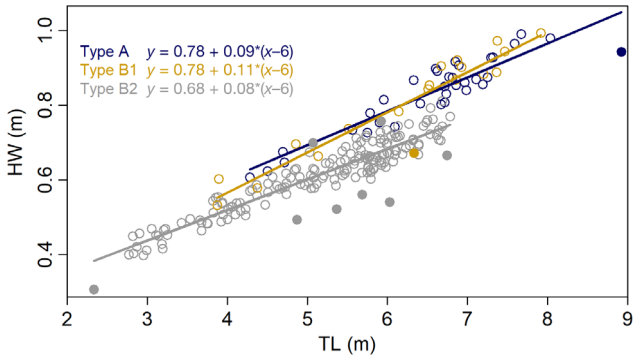

Fig. 5. Head width (HW, proxy for body condition) against total length (TL) for individual killer whales of Types A, B1 and B2 measured around the Antarctic Peninsula using aerial photogrammetry. Lines and equations show the model fit of a linear model for y = HW against x = TL centered on 6 m (x–6), based on median estimates of Bayesian posterior distributions. Outliers, shown by filled circles, are whales that had a high probability ($p > 0.75$) of a residual of >2 SD on either side of the regression line

Fig. 5). Three of these were adult females (Fig. 3) and 1 was a dependent calf of one of these females.

4. DISCUSSION

Data on body lengths are a key component for estimating the trophic requirements of killer whales and can therefore help to fill key data gaps on apex predators by parameterizing energetic models of trophic dynamics (e.g. Guénette et al. 2006). Specifically, their food requirements depend on body mass (Noren 2011), which scales non-linearly with body length (Bigg & Wolman 1975). We measured large differences in body length between the killer whale ecotypes found around the AP, with ecotype B2 being diminutive in length compared to the other ecotypes A and B1, which will translate into large differences in prey requirements. Adult females ranged in average size from 5.82 m in the small Type B2s to 6.93 m in the largest B1s, while adult males ranged in average size from 6.44 m (Type B2) to 7.80 m (Type A). These differences are even greater if we convert length to body mass due to the non-linear relationship (Bigg & Wolman 1975), which predicts that mass of average males would range from 3602 kg for Type B2 to 5902 kg for Type A, a difference of 2300 kg. However, this relationship was based on live-captured killer whales in the eastern North Pacific Ocean, and therefore does not fully account for the significant variation in body condition reported here between AP killer whale types.

Differences in body condition between the ecotypes informs nutritional health and provides important insight into population health (Stewart et al. 2021a). In particular, Type B2 killer whales were significantly leaner than the larger Types A and B1, even after controlling for body length differences. Although this may reflect natural shape differences between the ecotypes, divergent regression lines of HW~TL indicated that this difference was becoming even more pronounced at larger body sizes, with some anomalously thin adult female B2s, highlighting that the adults with higher energetic requirements (see Noren 2011, Fearnbach et al. 2018) were presenting in leaner body condition. This initially may seem contrary to recent abundance trends, which have documented Type B1s declining over the past decade, Type As increasing and Type B2s generally stable (Fearnbach et al. 2019, 2021). However, Type B2s are present around the AP in much higher abundance than the other killer whale types, with a population size approaching 1000 in recent years, compared to ~100 for B1s and ~150 for As (Fearnbach et al. 2019, 2021). As such, poorer body condition and smaller body sizes may represent density-dependent responses (e.g. Kasuya 1991) of a population close to carrying capacity, or the result of food limitation in a stable population as a result of acute environmentally driven changes in their carrying capacity (Moore et al. 2001).

More information is required on the relative contributions of different prey species to the diets of killer whale types around the AP, particularly Type B2, so we can better understand the predator–prey dynamics that define carrying capacity. However, well-documented environmental changes around the AP support the hypothesis of food limitation concurrent with our study. In addition to longer-term climate warming around the AP (Convey & Peck 2019), our study overlapped with a period of acute sea ice reduction and warmer ocean temperatures (Turner et al. 2020). Tight relationships between sea ice, primary production and abundance of marine herbivores, notably Antarctic krill *Euphausia superba*, suggest that these changes likely had major impacts on the pelagic food web on which killer whales depend (Gutt et al. 2021). Direct effects of sea-ice changes have also been documented for known or suspected prey of Type B2 killer whales, including ice-obligate penguin and Weddell seal populations (e.g. Chambert et al. 2012, Le Guen et al. 2018, Ropert-Coudert et al. 2018). Similarly, the keystone fish species, the Antarctic silverfish *Pleuragramma antarctica*, uses the sub-ice platelet layer as a nursery ground (Vacchi et al.

2017), and large reductions in the distribution of these ice-dependent silverfish have occurred on the western AP shelf (Parker et al. 2015), even prior to the recent acute reduction in sea ice.

Although Type B2 killer whales have generally been stable in abundance over the last decade (Fearnbach et al. 2021), our recent data on poor body condition may be predictive of future mortalities. Similar photogrammetry research has recently linked poor body condition to a subsequent increase in mortality for killer whales in the eastern North Pacific (Stewart et al. 2021a), documented poor body condition and constrained growth to be associated with declining abundance of North Atlantic right whales *Eubalaena glacialis* (Christiansen et al. 2020, Stewart et al. 2021b) and revealed reduced body condition associated with an unusual mortality event for eastern North Pacific gray whales *Eschrichtius robustus* (Christiansen et al. 2021). Of particular note, the anomalously low survival of Type B2 killer whales between 2015/16 and 2016/17 reported by Fearnbach et al. (2021) coincided with our documentation of Type B2 killer whales in relatively poor body condition, including the anomalously lean outliers. An extended time series of body condition data will further elucidate this apparent link between condition and population dynamics (e.g. Stewart et al. 2021a). As such, the new photogrammetry measurements presented here represent important baselines for monitoring future changes in the nutritional health of these apex predators in the face of climate-driven ecosystem dynamics.

Acknowledgements. All field work was conducted from small boat launches from Lindblad Expedition's ship MV 'National Geographic Explorer'. We are extremely grateful for support from the Lindblad-Expeditions-National Geographic (LEX-NG) Conservation Fund, from Amy Berquist from LEX, and from all onboard officers, crew and expedition staff. Particular thanks go to Captains Oliver Kruess and Leif Skog, and Expedition Leaders Lucho Verdesoto, Brent Stephenson, Jimmy White, Russ Evans and Lisa Trotter. Molly Groskreutz and Paige Casler assisted with laboratory photogrammetry measurements. Trevor Joyce, Jessica Farrer, Jimmy White, Doug Gaultieri, Paul North, Ian Tomcho, Eduardo Shaw and Bud Lehnhausen assisted ably in the field. The Pew Charitable Trusts and the LEX-NG Conservation Fund supported image analysis. Wayne Perryman, Bob Pitman, George Watters and Dave Weller provided useful comments on an earlier version of this manuscript. We are grateful for the helpful reviews by 3 anonymous reviewers, and for extremely useful suggestions by the handling editor, Robert Suryan. Research was authorized by Permits 14097 and 19091 from the US National Marine Fisheries Service and Antarctic Conservation Act Permits 2015-001 and 2017-029 from the US National Science Foundation.

LITERATURE CITED

Bestelmeyer BT, Ellison AM, Fraser WR, Gorman KB and others (2011) Analysis of abrupt transitions in ecological systems. Ecosphere 2:1–26

Bigg MA, Wolman AA (1975) Live-capture killer whale (*Orcinus orca*) fishery, British Columbia and Washington, 1962–73. J Fish Res Board Can 32:1213–1221

Chaloner K, Brant R (1988) A Bayesian approach to outlier detection and residual analysis. Biometrika 75: 651–659

Chambert T, Rotella JJ, Garrott RA (2012) Environmental extremes versus ecological extremes: impact of a massive iceberg on the population dynamics of a high-level Antarctic marine predator. Proc R Soc B 279: 4532–4541

Christiansen F, Dawson SM, Durban JW, Fearnbach H and others (2020) Population comparison of right whale body condition reveals poor state of the North Atlantic right whale. Mar Ecol Prog Ser 640:1–16

Christiansen F, Rodríguez-González F, Martínez-Aguilar S, Urbán J and others (2021) Poor body condition associated with an unusual mortality event in gray whales. Mar Ecol Prog Ser 658:237–252

Convey P, Peck LS (2019) Antarctic environmental change and biological responses. Sci Adv 5:eaaz0888

de Valpine P, Paciorek C, Turek D, Michaud N and others (2020) Nimble: MCMC, particle filtering, and programmable hierarchical modeling. R package version 0.9.1. https://CRAN.R-project.org/package=nimble

Durban JW, Pitman RL (2012) Antarctic killer whales make rapid, round-trip movements to subtropical waters: evidence for physiological maintenance migrations? Biol Lett 8:274–277

Durban JW, Fearnbach H, Barrett-Lennard LG, Perryman WL, Leroi DJ (2015) Photogrammetry of killer whales using a small hexacopter launched at sea. J Unmanned Veh Syst 3:131–135

Durban JW, Moore MJ, Chiang G, Hickmott LS and others (2016) Photogrammetry of blue whales with an unmanned hexacopter. Mar Mamm Sci 32:1510–1515

Durban JW, Fearnbach H, Burrows DG, Ylitalo GM, Pitman RL (2017) Morphological and ecological evidence for two sympatric forms of Type B killer whale around the Antarctic Peninsula. Polar Biol 40:231–236

Fearnbach H, Durban JW, Ellifrit DK, Balcomb KC (2018) Using aerial photogrammetry to detect changes in body condition of endangered southern resident killer whales. Endang Species Res 35:175–180

Fearnbach H, Durban JW, Ellifrit DK, Pitman RL (2019) Abundance of Type A killer whales (*Orcinus orca*) in the coastal waters off the western Antarctic Peninsula. Polar Biol 42:1477–1488

Fearnbach H, Durban JW, Barrett-Lennard LG, Ellifrit DK, Balcomb KC (2020) Evaluating the power of photogrammetry for monitoring killer whale body condition. Mar Mamm Sci 36:359–364

Fearnbach H, Durban JW, Ellifrit DK, Paredes A, Hickmott LS, Pitman RL (2021) A decade of photo-identification reveals contrasting abundance and trends of Type B killer whales in the coastal waters of the Antarctic Peninsula. Mar Mamm Sci, https://doi.org/10.1111/mms.12846

Foote AD, Morin PA, Durban JW, Pitman RL and others (2011) Positive selection on the killer whale mitogenome. Biol Lett 7:116–118

Foote AD, Vijay N, Ávila-Arcos MC, Baird RW and others (2016) Genome-culture coevolution promotes rapid divergence of killer whale ecotypes. Nat Commun 7:11693

Ford JK, Ellis GM, Olesiuk PF, Balcomb KC (2010) Linking killer whale survival and prey abundance: food limitation in the oceans' apex predator? Biol Lett 6:139–142

Gerrodette TM (1987) A power analysis for detecting trends. Ecology 68:1364–1372

Groskreutz MJ, Durban JW, Fearnbach H, Barrett-Lennard LG, Towers JR, Ford JKB (2019) Decadal changes in adult size of salmon-eating killer whales in the eastern North Pacific. Endang Species Res 40:183–188

Guénette S, Heymans SJ, Christensen V, Trites AW (2006) Ecosystem models show combined effects of fishing, predation, competition, and ocean productivity on Steller sea lions (*Eumetopias jubatus*) in Alaska. Can J Fish Aquat Sci 63:2495–2517

Gutt J, Isla E, Xavier JC, Adams BJ and others (2021) Antarctic ecosystems in transition—life between stresses and opportunities. Biol Rev (Camb) 96:798–821

Kasuya T (1991) Density dependent growth in North Pacific sperm whales. Mar Mamm Sci 7:230–257

Kéry M (2010) Introduction to WinBUGS for ecologists: Bayesian approach to regression, ANOVA, mixed models and related analyses. Academic Press, Cambridge, MA

Le Guen C, Kato A, Raymond B, Barbraud C and others (2018) Reproductive performance and diving behaviour share a common sea-ice concentration optimum in Adélie penguins (*Pygoscelis adeliae*). Glob Change Biol 24: 5304–5317

Moore SE, Perryman WL, Gulland F, Wade PR, Rojas-Bracho L, Rowles T (2001) Are gray whales hitting 'K' hard? Mar Mamm Sci 17:954–958

Morin PA, Archer FI, Foote AD, Vilstrup J and others (2010) Complete mitochondrial genome phylogeographic analysis of killer whales (*Orcinus orca*) indicates multiple species. Genome Res 20:908–916

Morin PA, Parsons KM, Archer FI, Ávila-Arcos MC and others (2015) Geographic and temporal dynamics of a global radiation and diversification in the killer whale. Mol Ecol 24:3964–3979

Noren DP (2011) Estimated field metabolic rates and prey requirements of resident killer whales. Mar Mamm Sci 27:60–77

Parker ML, Fraser WR, Ashford J, Patarnello T, Zane L, Torres JJ (2015) Assemblages of micronektonic fishes and invertebrates in a gradient of regional warming along the Western Antarctic Peninsula. J Mar Syst 152:18–41

Pitman RL, Durban JW (2010) Killer whale predation on penguins in Antarctica. Polar Biol 33:1589–1594

Pitman RL, Durban JW (2012) Cooperative hunting behavior, prey selectivity and prey handling by pack ice killer whales (*Orcinus orca*), type B, in Antarctic Peninsula waters. Mar Mamm Sci 28:16–36

Pitman RL, Ensor P (2003) Three forms of killer whales (*Orcinus orca*) in Antarctic waters. J Cetacean Res Manag 5: 131–140

Pitman RL, Durban JW, Joyce T, Fearnbach H, Panigada S, Lauriano G (2020) Skin in the game: epidermal molt as a driver of long-distance migration in whales. Mar Mamm Sci 36:565–594

Ropert-Coudert Y, Kato A, Shiomi K, Barbraud C and others (2018) Two recent massive breeding failures in an Adélie penguin colony call for the creation of a marine protected area in D'Urville Sea/Mertz. Front Mar Sci 5:264

Stewart JD, Durban JW, Fearnbach H, Barrett-Lennard LG, Casler PK, Ward EJ, Dapp DR (2021a) Survival of the fattest: linking body condition to prey availability and survivorship of killer whales. Ecosphere 12:e03660

Stewart JD, Durban JW, Knowlton AR, Lynn MS and others (2021b) Decreasing body lengths in North Atlantic right whales. Curr Biol 31:3174–3179.e3

Turner J, Guarino MV, Arnatt J, Jena B and others (2020) Recent decrease of summer sea ice in the Weddell Sea, Antarctica. Geophys Res Lett 47:e2020GL087127

Vacchi M, Pisano E, Ghigliotti L (2017) The Antarctic silverfish: a keystone species in a changing ecosystem. Springer International Publishing, Basel

Editorial responsibility: Robert M. Suryan, Juneau, Alaska, USA
Reviewed by: A. Friedlaender and 2 anonymous referees

Submitted: August 13, 2020
Accepted: August 9, 2021
Proofs received from author(s): October 2, 2021